MAX-PLANCK-GESELLSCHAFT

Keep it flexible:
Driving macromolecular rotary motions in atomistic simulations with GROMACS

Carsten Kutzner, Jacek Czub, and Helmut Grubmüller

Theoretical and Computational Biophysics, Max Planck Institute for Biophysical Chemistry, Göttingen, Germany

Abstract. Biomolecular function is often performed through motions of subunits. Rotary motions, in particular, are essential for the function of many motor proteins. Rotary mechanisms have been demonstrated, e.g., for the Fo and F1 motors in F-ATP synthase, and for the bacterial flagellar motor. The molecular mechanisms by which chemical reactions or transmembrane gradients drive protein rotary motions are in most cases not understood in full detail. Moreover, these motions are typically too slow or infrequent to be accessible to equilibrium molecular dynamics (MD) simulations. To overcome these limitations, external forces or torques can be imposed on specific subunits to induce rotation or to increase its rate. Using a simple fixed axis rotation (Fig. 1AB), however, does not reflect situations such as F1-ATP synthase (Fig. 1D), where the rotating part is flexible and adapts to the steric restraints of its bearing (Fig. 2C).

To more realistically describe biomolecular rotations, we have developed a new technique (→ Theory & Methods) that ***allows for flexible adaptions of both the rotary subunit as well as the local rotation axis*** during the simulation [1]. For the example of *γ* subunit rotation in F1-ATP synthase (Fig. 1D), we show that the flexible rotation method imposes minimal constraints on the rotor and allows for conformational adaptions to the surrounding (Fig. 3). This is confirmed by a 5-fold reduced torque when using our flexible axis compared to a fixed axis rotation at the same rotation rate (Figs. 4-5).

The flexible axis technique can be used, e.g., to mimic rotary molecular motors, to restrain the orientation of a protein or ligand, or, in combination with umbrella sampling, to calculate the preferred orientation of transmembrane proteins within a lipid bilayer. We have implemented flexible axis enforced rotation for the Gromacs 4.6 MD package [2]. The flexible axis approach allows to simulate various rotation-related phenomena on MD time scales with minimal restrictions on the rotated parts.

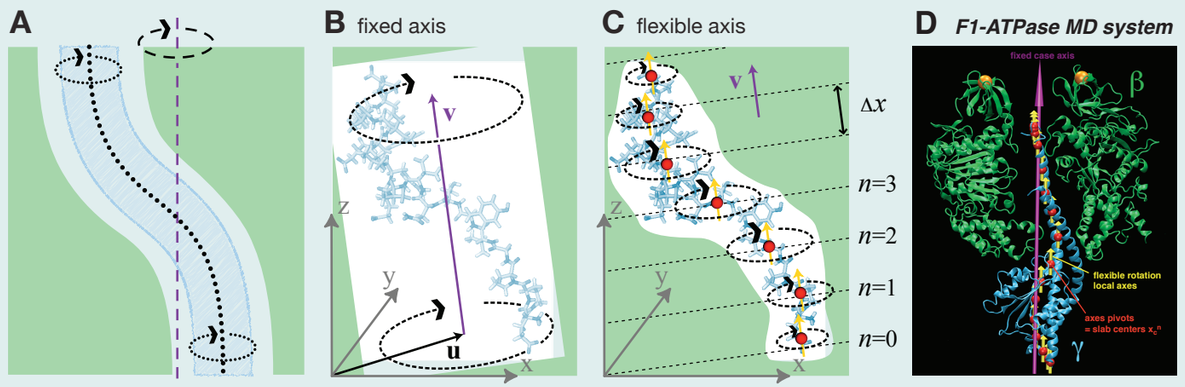

Fig. 1 ***Comparison of fixed and flexible axis rotation.*** *(A) Rotating the **sketched blue shape** inside the green cavity creates severe artifacts when a **conventional fixed rotation axis (dashed)** is used. More realistically, the shape would revolve like a flexible pipe-cleaner (dotted) inside the bearing.* *(B) Fixed rotation around an **axis v** with a pivot **u**.* *(C) Subdividing the rotating fragment into slabs with separate rotation axes (') and pivots (•) allows for the required flexibility.* *(D) F1-ATPase MD simulation system with a **fixed** and a flexible axis (yellow/red).*

Theory & Methods.

To enforce rotation, a subset of N atoms is subjected to a potential V. Each atom at position $\boldsymbol{x}_i$ gets assigned an equilibrium position $\boldsymbol{y}_i(t)$, which is derived by rotating a reference position $\boldsymbol{y}_i^0$ at constant angular rate ω about an axis $\boldsymbol{v}$. The initial positions may serve as $\boldsymbol{y}_i^0$. The »isotropic« ***fixed axis*** potential (Figs. 1B & 6A)

$$V^{\text{iso}} = \frac{k}{2}\sum_{i=1}^{N} w_i \left[\boldsymbol{\Omega}(t)(\mathbf{y}_i^0 - \mathbf{u}) - (\mathbf{x}_i - \mathbf{u})\right]^2$$

with the rotation matrix $\Omega(t)$ and the pivot $\boldsymbol{u}$ of the axis yields forces towards the (rotating) equilibrium positions $\boldsymbol{y}_i(t)$, thereby effectively rotating $\boldsymbol{x}_i$. Optionally, with the prefactors $w_i = N\,m_i/M$, total mass M, mass-weighting can be achieved.

Starting from the fixed axis potential V^{iso} we develop the flexible axis rotation in 4 steps, each of which removes one of the restraints inherent in this simple potential.

I. Detach the pivot.

A translation-invariant pivot is achieved by selecting the rotor center of mass $\mathbf{x}_c$ as the pivot (instead of $\boldsymbol{u}$):

$$\mathbf{x}_c = \frac{1}{M}\sum_{i=1}^{N} m_i \mathbf{x}_i \qquad \mathbf{y}_c^0 = \frac{1}{M}\sum_{i=1}^{N} m_i \mathbf{y}_i^0$$

This results in the »pivot-free« potential

$$V^{\text{iso-pf}} = \frac{k}{2}\sum_{i=1}^{N} w_i \left[\boldsymbol{\Omega}(\mathbf{y}_i^0 - \mathbf{y}_c^0) - (\mathbf{x}_i - \mathbf{x}_c)\right]^2$$

II. Apply only angular restraints.

For V^{iso} and $V^{\text{iso-pf}}$ the potential minimum is a single point at the position of the reference, thereby any radial deviation from the reference conformation is penalized. The »radial motion« potential (Fig. 3B) does not constrain atoms at their equilibrium angular position:

$$V^{\text{rm-pf}} = \frac{k}{2}\sum_{i=1}^{N} w_i \left[\frac{\hat{\mathbf{v}} \times (\mathbf{y}_i^0 - \mathbf{y}_c^0)}{\|\hat{\mathbf{v}} \times (\mathbf{y}_i^0 - \mathbf{y}_c^0)\|} \cdot (\mathbf{x}_i - \mathbf{x}_c)\right]^2$$

The following slightly advanced variant (Fig. 3C) yields forces perpendicular to the radial position only, thus not expdanding or contracting the structure as in Fig. 3B:

$$V^{\text{rm2-pf}} = \frac{k}{2}\sum_{i=1}^{N} w_i \frac{\left[(\hat{\mathbf{v}} \times (\mathbf{x}_i - \mathbf{x}_c)) \cdot \boldsymbol{\Omega}(\mathbf{y}_i^0 - \mathbf{y}_c)\right]^2}{\|\hat{\mathbf{v}} \times (\mathbf{x}_i - \mathbf{x}_c)\|^2 + \epsilon'}$$

A small positive ε' yields well-defined forces also in the vicinity of the pivot (Fig. 3D).

III. Segment into »soft« slabs.

Now the rotor is partitioned into equidistant slabs $\perp$ to $\boldsymbol{v}$ (Fig. 1C). Discontinuities are avoided by using »soft« slabs by weighing the contributions to V from each slab by a Gaussian function (Fig. 7)

$$g_n(\mathbf{x}_i) = \gamma\,\exp\left(-\frac{\beta_n^2(\mathbf{x}_i)}{2\sigma^2}\right)$$

centered at the midplane of slab n. σ is the width of the Gaussian, Δx the slab distance and

$$\beta_n(\mathbf{x}_i) := \mathbf{x}_i \cdot \hat{\mathbf{v}} - n\,\Delta x$$

We define the instantaneous slab centers (=local slab axis pivots, red in Fig. 1D) as

$$\mathbf{x}_c^n = \frac{\sum_{i=1}^{N} g_n(\mathbf{x}_i)\, m_i\, \mathbf{x}_i}{\sum_{i=1}^{N} g_n(\mathbf{x}_i)\, m_i}$$

and the reference slab centers correspondingly.

IV. Sum up all slabs' contributions.

Finally, we can apply the Gaussian slab segmentation to any of the above potentials and sum up the contributions from all slabs, yielding a smooth potential with continuous forces everywhere. If applied to $V^{\text{rm-pf}}$ the ***»flexible«*** potential results:

$$V^{\text{flex}} = \frac{k}{2}\sum_{n}\sum_{i=1}^{N} w_i\, g_n(\mathbf{x}_i) \left[\frac{\hat{\mathbf{v}} \times \boldsymbol{\Omega}(\mathbf{y}_i^0 - \mathbf{y}_c^n)}{\|\hat{\mathbf{v}} \times \boldsymbol{\Omega}(\mathbf{y}_i^0 - \mathbf{y}_c^n)\|} \cdot (\mathbf{x}_i - \mathbf{x}_c^n)\right]^2$$

For $V^{\text{rm2-pf}}$ the ***»flexible 2«*** potential results:

$$V^{\text{flex2}} = \frac{k}{2}\sum_{i=1}^{N}\sum_{n} w_i\, g_n(\mathbf{x}_i) \frac{\left[(\hat{\mathbf{v}} \times (\mathbf{x}_i - \mathbf{x}_c^n)) \cdot \boldsymbol{\Omega}(\mathbf{y}_i^0 - \mathbf{y}_c^n)\right]^2}{\|\hat{\mathbf{v}} \times (\mathbf{x}_i - \mathbf{x}_c^n)\|^2 + \epsilon'}$$

Results.

To test whether our flexible axis approach is capable of providing more accurate torque or free energy profiles, we apply fixed and flexible axis rotation to the 272 Cα carbons of the F1-ATPase *γ* rotor. For simulation details, see [1].

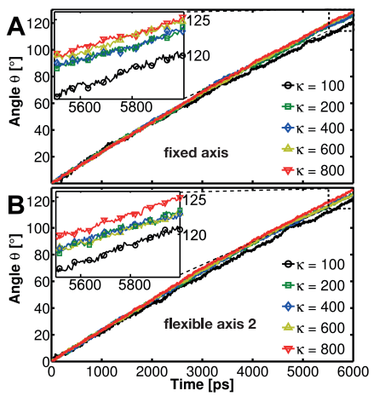

Fig. 2 *Time evolution of the γ rotor angle when enforcing the F1 motor to rotate in the synthesis direction at a rate of 0.021°/ps. For all rotation types the rotor angle closely follows the requested angular velocity.*

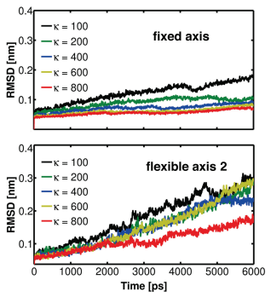

Fig. 3 *RMSD of the γ rotor backbone atoms with respect to the X-ray structure for the F1 motor driven in synthesis direction using various spring constants k. In contrast to fixed rotation, the flexible approach allows for structural rearrangements, as also seen in Fig. 5B.*

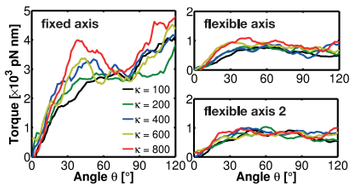

Fig. 4 *Angular dependence of the driving torque for the γ rotor driven in synthesis direction using the fixed/flexible/flexible2 potentials with various spring constants k. The average torque along θ is ≈ 5× smaller with a flexible axis, therefor also the dissipated energy is reduced drastically.*

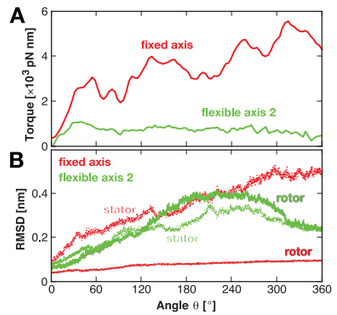

Fig. 5 *(A) as Fig. 4, but for a whole 360° rotation at k=600 kJ/(mol nm²). (B) RMSD of the γ rotor backbone atoms (solid) and of the $\alpha_3\beta_2$ bearing (dotted) with respect to the X-ray structure. While fixed axis rotation induces structural changes mostly in the bearing, in the flexible case the structural changes are distributed evenly among rotor and stator. Only in the flexible case the starting structure is approached after 360° rotation.*

References.

[1] C Kutzner, J Czub, H Grubmüller, 2011. Keep it Flexible: Driving Macromolecular Rotary Motions in Atomistic Simulations with GROMACS. JCTC 7: 1381-1393.

[2] B. Hess, C. Kutzner, D. van der Spoel, E. Lindahl, 2008. GROMACS 4: Algorithms for highly efficient, load-balanced, and scalable molecular simulation. JCTC 4: 435–447.

[3] www.mpibpc.mpg.de/home/grubmueller/projects/Methods/Rotation

Fig. 6 *Visualization of the rotation potentials. Shown is $e^{-V/(k_B T)}$ in a plane ⊥ to v for T=300K and k=200 kJ/(mol nm²). Green arrows, force on atom j.*

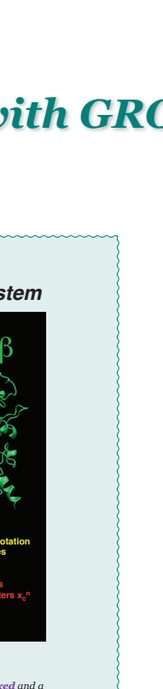

Fig. 7 *Gaussians g_n used for the smooth slab decomposition. (Here, Δx=1.5 nm, σ = 0.7Δx and γ=1/1.7547).*